Progress in Physics of Applied Materials 3 (2023) 159–168

Semnan University

Progress in Physics of Applied Materials

journal homepage: https://ppam.semnan.ac.ir/

Strategies to Improve Photovoltaic Performance of "Green" $CuInS_2$ Quantum Dots

A. Jamshidi Zavaraki [a], J. Huang[b], B. Xu[c], L. Sun[c], H. Ågren[d]

[a] *Faculty of New Sciences and Technologies, University of Tehran, North Kargar Street, Tehran, Iran*
[b] *Departments of Theoretical Chemistry & Biology, School of Biotechnology, Royal Institute of Technology (KTH), Stockholm, Sweden*
[c] *Organic Chemistry, Centre of Molecular Devices, Department of Chemistry, School of Chemical Science and Engineering, Royal Institute of Technology (KTH), Stockholm, Sweden*
[d] *Departments of Physics and Astronomy, Uppsala University, Uppsala, Sweden*

ARTICLE INFO

Article history:
Received: 6 November 2023
Revised: 16 December 2023
Accepted: 18 December 2023

Keywords:
Colloidal quantum dot
Synthesis
Sensitized solar cell
Passivation

ABSTRACT

While nanocrystals in group II-IV semiconductors have been extensively studied as photosensitizers in quantum dot-sensitized solar cells (QDSCs), their practical use is severely hampered by the high toxicity of the heavy metals, like Cd, Pb, and Hg, present in these semiconductors. Our present work is based on a proposition to use a "green" alternative to the currently used sensitizers, namely $CuInS_2$ which is a low-toxic semiconductor. However, as for many other types of QDs, surface defects limit also their photovoltaic performance. Therefore, in order to passivate the surface defects and improve the performance of $CuInS_2$ QDs we explore in this work two strategies - ZnS shell coating and hybrid passivation. The results show that although ZnS shell coating can effectively passivate the surface defects, the electron injection from QDs to TiO_2 nanoparticle is also hampered. Moreover, the size of $CuInS_2$ QDs is increased after the shell coating, which also is unfavorable for the enhancement of the solar cells efficiency. In contrast, hybrid passivation can passivate the surface defects on the $CuInS_2$ QDs without size changing, and can increase the loading efficiency of the QDs simultaneously. Consequently, the efficiency of the solar cells is improved to 4.7%, which is a promising result for the green $CuInS_2$ based QDSCs. Therefore, in addition to the most used shell coatings of $CuInS_2$ QDs, hybrid passivation may be an effective way for improving their photovoltaic performance. This study employs two strategies "hybrid passivation and ZnS shell coating" and discuss about their effect in solar cell efficiency.

1. Introduction

Beside perovskites [1-2], Colloidal quantum dots (QDs) have attracted intensive attention in recent years, due to their promising applications in areas like renewable energy[3-4], light emission [5], biomedical area [6]. Benefitting from their tunable light absorption, high extinction coefficient [7], potential multiple exciton generation (MEG), photostability low-cost materials and easy production [8], colloidal QDs have been employed in quantum dot-sensitized solar cells (QDSCs), which possess the maximum theoretical power conversion efficiency (PCE) of 44% [9-10] and have been considered as promising candidates for the next-generation photovoltaics [11].

Different types of QDs such as type I core/shell [12-15], type II core/shell [16-18], alloyed [19-22] QDs have been widely employed as sensitizers in QD sensitized solar cells. Recently, solar cells based on colloidal QDs have indeed achieved great progress in terms of PCE. The PCE of depleted heterojunction cells with colloidal PbS QDs has reached 9.2% [23]. Zhao et al. improved the PCE of QDSCs to 8.21% with colloidal alloyed CdSeTe QDs, which is the highest efficiency for QDSCs until now [24]. However, most of the common QDs used in QDSCs are based on heavy

* Corresponding author.
E-mail address: jamshidi.zavaraki@ut.ac.ir

Cite this article as:
Jamshidi Zavaraki A., Huang J., Xu B., Sun L. and Ågren H., 2023. Strategies to Improve Photovoltaic Performance of "Green" $CuInS_2$ Quantum Dots. *Progress in Physics of Applied Materials*, *3*(2), pp.159-168. DOI: **10.22075/PPAM.2023.32263.1068**

metals, such as Pb, Cd, Hg, which are not eco-friendly and restrict the commercialization of the QDSCs. $CuInS_2$, which is less toxic, can be a promising alternative semiconductor to the Cd- and Pb-based QDs, due to their similar photoelectrical properties - small band gap of 1.5 eV, high absorption coefficient ($\sim 10^5$) and good chemistry stability. In addition, the easy solution-processed preparation of $CuInS_2$ QDs offers a cost reduction for fabrication of the QDSCs.

$CuInS_2$-based QDs have been investigated and employed as sensitizers for improvement of efficiency in dye-sensitized solar cell [25-26], perovskite solar cell [27], polymer-based solar cell [28] and Si-based solar cell [29]. In case of QDSCs, different strategies such as ZnSe- coating layer [30], interfacial buffer layer [31], Mn doping with CdS shell coating [32] has been used to enhance the efficiency of $CuInS_2$-based QDSCs. Recently, a certified efficiency of 6.66% was obtained with colloidal $CuInS_2$/ZnS QDs for QDSCs, which is the best result for "green" QDSCs so far [33]. However, the photovoltaic performance of colloidal $CuInS_2$ QDs in QDSCs still cannot be comparable with the Cd- and Pb-based QDs.

Surface defects on the QDs, which will trap excitons and induce recombination of charge carriers in the device, can be part of the reasons that account for the low photovoltaic performance of $CuInS_2$ QDs. As a compound from the ternary I-III-VI group, chalcopyrite $CuInS_2$ semiconductors can tolerate a large range of cation and anion off-stoichiometry, and create extensive intrinsic defects [34]. According to a debate in the literature, there are two kinds of defects associated to $CuInS_2$ QDs - internal defects and surface defects [35-37]. The internal defects, usually related to Cu vacancies, can significantly influence the fluorescence peak and promote the emission intensity of $CuInS_2$ QDs. The surface defects, originating from dangling bonds and imperfect surface atomic termination, always induce non-radiative recombination of the excitons in the excited $CuInS_2$ QDs [35-37]. Due to the abundant surface defects, the photoluminescence quantum yield (PLQY) of $CuInS_2$ QDs is always low, and researchers tend to passivate the surface of $CuInS_2$ QDs with inorganic shells, such as CdS and ZnS, to enhance the PLQY [38-39]. Similarly, shell coating with CdS or ZnS has also been reported to improve the photovoltaic performance of $CuInS_2$ QDs in QDSCs. In early studies, the colloidal $CuInS_2$ QDs were attached on the photoelectrodes, followed by coating the electrodes with a CdS layer, so greatly improving the PCEs of the QDSC [40-41]. Subsequently McDaniel et al used zinc oleate and cadmium oleate to treat the pre-synthesized CuInSeS QDs to passivate the surface defects, which significantly enhanced the efficiency of the QDSCs, with the efficiency reaching 5.13% [42]. Recently, Zhang et al applied shell coating on both $CuInS_2$ QDs and $CuInSe_2$ QDs to form $CuInS_2$/ZnS and $CuInSe_2$/ZnS core/shell QDs, and acquired "green" QDSCs with high efficiency, which exceeded 6% in both cases [38].

Apart from shell coating, introducing atomic ligands with halide ions is another effective approach to passivate the surface of colloidal QDs. Sargent et al employed halide ion passivation to colloidal PbS QDs to considerably improve the performance of hereojunction quantum dot solar cells [43-44]. Our previous work established hybrid passivation, through combining the ligand of MPA and iodide ions to colloidal CdSe QDs, successfully increased the loading efficiency of QDs and reducing the surface defects on QDs. An enhanced efficiency of the QDSCs was thereby achieved [45].

In order to find a better strategy to passivate the surface defects and improve the photovoltaic performance of $CuInS_2$ QDs, both hybrid passivation and ZnS shell coating are, in this work, tested on $CuInS_2$ QDs. Comparisons between these two kinds of improving strategies indicate that though ZnS shell coating indeed can passivate the surface of $CuInS_2$ QDs and reduce the interface recombination in the device, it does not favor the performance of the resultant QDSCs. In contrast, hybrid passivation not only passivates the surface of the $CuInS_2$ QDs, but also significantly enhances the efficiency of the $CuInS_2$ based QDSCs, up to 4.7%.

2. Experimental

2.1. Chemicals

Copper iodide (CuI, ≥99.5%), zinc acetate (Zn Ff$(OAc)_2$, 99.99%), oleylamine (OAm, 97%), 3-mercaptopropionic acid (3-MPA, >99%) and tetrabutylammonium iodide (TBAI, 98%) were purchased from Sigma-Aldrich. Indium acetate (In $(OAc)_3$, 99.99%), sulfur powder (S, 99.5%), oleic acid (OA, 90%) and 1-octadecene (ODE, 90%) were purchased from Alfa Aesar. All chemicals were used as received.

2.2. Synthesis of $CuInS_2$ QDs

Synthesis of $CuInS_2$ QDs was based on previously published procedure. Briefly, 29 mg of $In(OAc)_3$ and 14 mg of CuI, 4 mL of ODE and 2 mL of OAm were mixed at 60 °C in a three neck flask under vacuum, and then 0.4 mL of sulfur precursor solution (1 M), prepared by dissolving sulfur powder in OAm at room temperature, was injected into the three necked flask after the mixture solution was heated to 180 °C under Ar flow. When the reaction solution kept at 180 °C for 20 min, the heater was removed to terminate the reaction. For purification, the obtained nanocrystals were precipitated with acetone, and then washed by repeating the dispersion in toluene and precipitation with addition of acetone.

2.3. ZnS Shell Coating

For the shell coating with ZnS layer, the purified $CuInS_2$ QDs were dispersed in 4.0 mL ODE and 2.0 mL OAm, and then was heated to 100 °C before implementing the vacuum at 40 °C for 20 min. 0.3 mL Zn-stock solution, prepared by dissolving 22 mg $Zn(OAc)_2$ in 0.08 mL OAm and 0.92 mL ODE at 150 °C, was then swiftly injected into the reaction system and kept at 100 °C for 10 min or 20 min to obtain different thickness of ZnS shell. These two kinds of $CuInS_2$ QDs with ZnS shell coating will be referred as Zn-10 QDs and Zn-20 QDs, respectively. After purification, the obtained Zn-10 and Zn-20 QDs were treated by ligand exchange reaction as described in below.

2.4. Ligand Exchange of $CuInS_2$ QDs

The ligand exchange reaction was carried out for all the $CuInS_2$ QDs, to make the QDs water soluble. Specifically, MPA ligand solution, formed by dissolving 0.3 mL MPA into 0.7 mL methanol, with the pH of the solution adjusted to the value of 12 by 40% NaOH solution, was dropped into 5 mL $CuInS_2$ QDs stock solution (10 mM, dispersing in toluene solution) under strong stirring. After stirring for 40 min, MPA capped QDs separated in the lower part, were collected and washed by water and acetone, and finally dispersed in deionized water for future use.

2.5. Hybrid Passivation of $CuInS_2$ QDs

The hybrid passivation procedure was based on our previously published report [45]. For the hybrid passivation of $CuInS_2$ QDs, 10 mg of TBAI was added to the above MPA ligand solution, and then similar ligand exchange reaction was conducted.

2.6. Fabrication of $CuInS_2$ QD-Sensitized solar cells

FTO (Fluorine Tin Oxide) conductive glass was used as substrate. Two transparent and scattering layers of TiO_2 mesoporous nanoparticles made from commercial paste (Solaronix) were deposited on 0.25 cm^2 of FTO by screen printing technique. The thickness of transparent layer (Ti-Nanoxide T/SP) and scattering layer Ti-Nanoxide R/SP) were estimated to be 7 and 4 μm, respectively. After TiO_2 deposition, the photoanodes were annealed at 500°C for 30 min.

The sintered electrodes were post-treated by aqueous $TiCl_4$ solution (40 mM) at 70 °C for 40 min. The QD-sensitized photoanode was obtained by pipetting 100 μL of $CuInS_2$ aqueous solution (0.017 M) onto the TiO_2 electrode, and the solution was left for 2 h in open air followed by removing the excess of $CuInS_2$ QDs by rinsing with water. This procedure was repeated once to increase the loading amount of QDs. After the deposition, the QD-sensitized TiO_2 electrode was treated with two circles of ZnS, by immersing the photoanode into $Zn(NO_3)_2$ aqueous solution (0.1 M) and Na_2S aqueous solution (0.1 M) for 1 min/dip alternately.

The Cu_2S counter electrodes were prepared by immersing polished brass foils into HCl solution (37%) at 80 °C for 10 min, and treated by polysulfide electrolyte solution for 10 min. The polysulfide solution was composed of 2 M S, 2 M Na_2S and 0.2 M KCl in a methanol–water (v/v, 3/7) solution. The solar cell was constructed by assembling a QD-sensitized photoanode and a Cu_2S counter electrode using a Surlyn film (50 μm), and then the polysulfide electrolyte was injected by vacuum backfilling through the hole preconstructed on top of the counter electrode.

2.7. Characterization

Transition electron microscopy (TEM) (Hitachi HT7700 microscope at 100 kV, equipped with energy-dispersive X-ray (EDX) spectra were recorded on a JEOL JEM-2100 microscope at 200 kV) was employed to analyze the QDs quality. Powder X-ray diffraction (XRD) patterns (X'Pert PANalytical PRO MRD using CuKα1 radiation (λ = 1.54056 Å)) was used to investigate the crystallinity of the QDs. UV-Vis absorption spectra (Lambda 750 UV-Vis spectrophotometer) and Fluorescence spectra (Ocean Optics with spectrometer of USB4000-UV-VIS-ES) were used for optical characterization (the excitation wavelength = 510 nm). All solution samples were measured in a 1 cm^2 cell at room temperature. TiO_2 film with only transparent layer on FTO glass was used for absorption measurement of QDs sensitized TiO_2 film. Current-Voltage (CV) characteristics were carried out by applying an external potential bias to the device while recording the generated photocurrent with a Keithley model 2400 digital source meter. The light source was a 300 W xenon lamp (Newport) calibrated with the light intensity to 100 mW/cm^2 at an AM 1.5 G solar light conditions by a certified silicon solar cell (Fraunhofer ISE). A mask of 0.25 cm^2 was used during the CV characterization. IPCE measurements were operated on a computer-controlled setup comprised of a xenon lamp (Spectral Products ASB-XE-175), a monochromator (Spectral Products CM110) and a potentiostat (EG&G PAR 273). The setup was calibrated with a certified silicon solar cell (Fraunhofer ISE) prior to measurements. Impedance spectroscopy (IS) was investigated with an impedance module from Autolab PGstat12 potentiostat.

3. Results and discussion

3.1. Characterization of colloidal $CuInS_2$ QDs and their original photovoltaic performance

Colloidal $CuInS_2$ QDs were synthesized by procedure similar to one explained in the literature [31], which facilitates the $CuInS_2$ QDs to load onto the photoanode by an effective linker-assisted assembly approach. The TEM image in Figure 1A shows that the as-synthesized $CuInS_2$ QDs exhibits a size range of 7.0±0.5 nm with pyramidal shape, arising from preferential evolution from Ostwald ripening of tetragonal chalcopyrite structure of $CuInS_2$, which is proven by the X-ray diffraction (XRD) pattern given in the Supporting Information (Figure S1). Absorption and photoluminescence (PL) spectra of the obtained $CuInS_2$ QDs are presented in Figure 1B. The absorption spectrum of the $CuInS_2$ QDs presents a shoulder around 750 nm with a long tail extending to 850 nm.

Such a broad absorption region makes the $CuInS_2$ QDs promising sensitizers for the TiO_2 electrodes in solar cells. Though fluorescence can be detected from the as-synthesized QDs, the PL quantum yield (QY) is quite low, almost zero. Low PL density of the obtained $CuInS_2$ QDs indicates the existence of numerous surface defects on the $CuInS_2$ QDs, which will jeopardize the photovoltaic performance of the colloidal $CuInS_2$ QDs in solar cells. The $CuInS_2$ QDs were ligand exchanged by MPA after the synthesis procedure, to make the QDs water soluble and more efficiently attachable to the TiO_2 film electrode through the bifunctional molecule MPA [44]. Figure 1C shows the photovoltaic performance of the $CuInS_2$ QDs when they were employed in the QDSCs as sensitizers, with Cu_2S counter electrode and polysulfide electrolyte. With the broad absorbance of the obtained $CuInS_2$ QDs and the effective linker-assisted deposition, the photocurrent (J_{sc}) of the device reached as much as 12.67 mA/cm^2, with the open-circuit voltage (V_{oc}) of 0.535 V and the fill factor (FF)

of 0.544, which made the overall power conversion efficiency (PCE) to amount to 3.7%.

The efficiency obtained by our colloidal $CuInS_2$ QDs is higher than most of other QDSCs based on only $CuInS_2$ QDs which are prepared from the successive ionic layer adsorption and reaction (SILAR) and chemical bath deposition (CBD) methods, however, the obtained $CuInS_2$ QDs still cannot compete with colloidal Pb based and Cd based QDs in the third generation solar cells. One reason for this maybe the high density surface defects on the $CuInS_2$ QDs, which can cause serious charge carriers recombination in the devices and degrade the performance of the solar cells. As proven by the weak fluorescence of the $CuInS_2$ QDs, surface defects are a major problem. In this work, we explore two different approaches to reduce the surface defects – ZnS shell coating and hybrid passivation. Comparison of these two methods will be discussed.

ZnS shell coating of the $CuInS_2$ QDs was realized via a cation exchange route. In order to get different thickness of the ZnS shell, reaction times of 10 min and 20 min were considered, and the resulting $CuInS_2$/ZnS QDs will be denoted as Zn-10 and Zn-20, respectively. As shown in Figure 2, the signal of Zn in energy-dispersive X-ray (EDX) spectra of Zn-20 can be clearly detected, while it is not obvious for Zn-10. In EDX spectra, the Zn peak is overlapped with Cu peak, which arose from the copper grid used in the measurement, therefore, the Zn peak will be merged by Cu peak when the content of Zn is low. Inductively coupled plasma atomic emission spectroscopy (ICP-AES) also shows that the Zn content in Zn-10 is lower than that in Zn-20, which is caused by shorter reaction time, and that the Zn content in both of the samples are lower than 20%. Hybrid passivation by MPA and iodide ions was carried out to the as-synthesized $CuInS_2$ QDs through ligand exchange reaction, following our previous report [43]. The appearance of I signal, together with S peak in the spectrum demonstrate that the $CuInS_2$ QDs were successfully hybrid passivated.

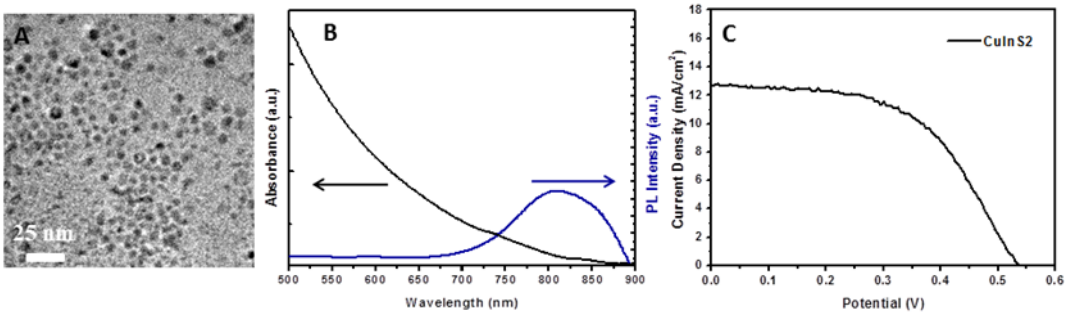

Fig. 1. TEM image (A), absorbance and fluorescence spectra (B) of the as-synthesized $CuInS_2$ QDs. (C) J-V curve of the colloidal $CuInS_2$ based QDSC.

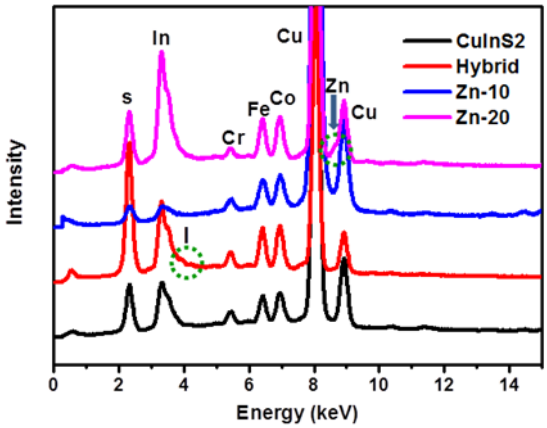

Fig. 2. EDS spectra of $CuInS_2$ QDs with different passivation. All of the samples were measured after ligand exchange reaction.

3.2. Fluorescence

Fig. 3 shows the fluorescence spectra of the $CuInS_2$ QDs with ZnS shell coating before ligand exchange with MPA. Similar to earlier works, the overcoating of ZnS resulted in a significant improvement of the PL intensity, and with prolongation of the reaction time, the fluorescence intensity became higher. Numerous studies have demonstrated that shell coating could minimize the fast, non-radiative decay in the excited $CuInS_2$ QDs due to role of ZnS as barrier, which are associated with the surface state, therefore longer PL lifetime and higher PL intensity could be obtained in core/shell $CuInS_2$/ZnS QDs. In other words, through the intensified emission, we believe that the surface defects on the $CuInS_2$ QDs were suppressed by ZnS shell coating, and that a thicker ZnS shell layer is more effective in the elimination of surface defects. In addition, the growth of ZnS shell leads to a blue shift of the PL peak, which may indicate the core material was etched to some extent under shell growth [38] or it could be ascribed to a partial alloying of $CuInS_2$ QDs with wide band gap ZnS layer [33]. Due to the hole extracting effect of the thiol group in MPA, the fluorescence was hardly detected in the hybrid passivated $CuInS_2$ QDs. No obvious change in absorption of $CuLnS_2$ was observed for the two strategies of ZnS shell coating and hybrid passivation.

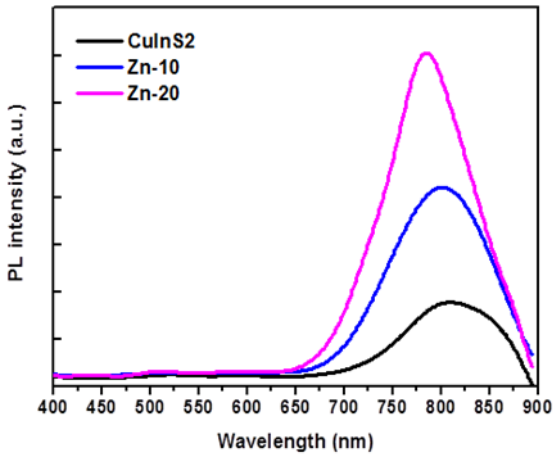

Fig. 3. Fluorescence spectra of $CuInS_2$ QDs solution and $CuInS_2$ QDs with ZnS shell coating solution.

3.3. Loading efficiency

The loading amount of the QDs on the photoanode plays an essential role for the performance of QDSCs, as it directly decides the photocurrent of the solar cells through light harvesting and indirectly influences the interfacial recombination in the devices. The work of McDaniel et al. shows high QDSC performance as they may benefit from the high surface coverage of the colloidal QDs on the photoanodes [42]. Therefore, the loading efficiency of the QDs is an important factor when we consider the photovoltaic performance of colloidal QDs. In our work, all types of $CuInS_2$ QDs have undergone ligand exchange reactions to make the QDs water soluble. The ligand MPA of these hydrophilic QDs promotes their tethering onto the TiO_2 nanoparticles. The same amount of aqueous solution of the $CuInS_2$ QDs with the same concentration was pipetted on the TiO_2 film electrodes in order to fabricate the sensitized photoanodes.

To evaluate the loading efficiency of the QDs, the absorbance of the sensitized TiO_2 films without any scattering layer was measured. As shown in Figure 4, compared to pristine $CuInS_2$ QDs, hybrid passivation slightly increases the absorbance of the sensitized TiO_2 films, which is similar to the previous result, while ZnS shell coating made the absorbance of the sensitized TiO_2 films lower.

Normally, deposition of colloidal QDs on TiO_2 film electrodes can be influenced by the size, shape, and type of surface ligands of the QDs, as well as by the solvent surrounding the QDs. Through TEM images of different kinds of $CuInS_2$ QDs one can find that the hybrid passivated $CuInS_2$ QDs keep a similar size as the plain $CuInS_2$ QDs (around 7 nm), while ZnS shell coating makes the QDs size increase. Here the size of Zn-10 was around 8 nm and Zn-20 showed even bigger size (almost 8.5 nm). Hence, the lower loading efficiency of the shell coated $CuInS_2$ QDs can be explained by the larger size of the QDs because it is then difficult for the QDs to penetrate into the mesoporous oxide film. On the other hand, the enhancement in loading efficiency for the hybrid passivated $CuInS_2$ QDs should not origin from the similar size of the QDs, but is probably related to the surface ligand of the QDs. Due to the small size of the iodide ions, the ligand exchange in hybrid passivation is more thorough than that with just MPA, and can remove the original capping ligand OAm more completely. Therefore, hybrid passivation is more beneficial for the $CuInS_2$ QDs to be deposited on TiO_2 film electrodes.

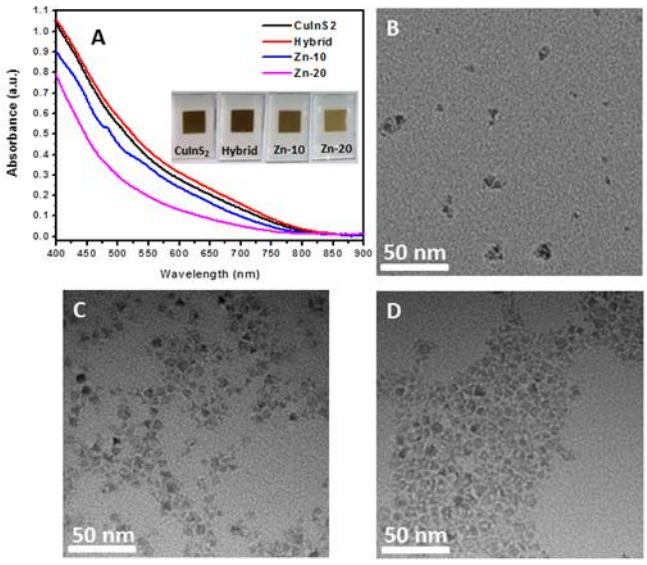

Fig. 4. (A) UV-Vis absorption spectra of sensitized TiO_2 electrodes based on $CuInS_2$ QDs with different passivation, and the corresponding photographs are inserted. TEM images of $CuInS_2$ QDs with hybrid passivation (B), $CuInS_2$ QDs with ZnS shell coating for 10 min (C), and $CuInS_2$ QDs with ZnS shell coating for 20 min (D).

3.4. IPCE and APCE

Subsequently the four types $CuInS_2$ QDs were employed in a typical QDSCs configuration, in which the Cu_2S counter electrodes and polysulfide electrolyte was used. The incident photon-to-carrier efficiency (IPCE) of solar cells, which also is known as the external quantum efficiency (EQE), is commonly used to describe how efficiently the incoming incident photons are converted to electrons, and provides a helpful measure to quantify sensitizers in QDSCs. In order to get information on the quantum efficiency of the QDs, the IPCE of the solar cells based on different $CuInS_2$ QDs are plotted in Figure 5A. The corresponding absorbed photon-to-electron conversion efficiency (APCE), which excludes the effect of different absorbance of the photoanodes due to the varied loading efficiency of the different $CuInS_2$ QDs, is calculated and shown in Figure 5B.

Compared to the original $CuInS_2$ QDs, the solar cells based on hybrid passivated $CuInS_2$ QDs shows both significantly improved IPCE and APCE values over the whole responsive region, indicating that hybrid passivation of the $CuInS_2$ QDs enhances the electron transfer efficiency in the solar cells (including both quantum yield of charge injection, ϕ_{inj}, and collection efficiency at the back contact, η_{cc}). This can be attributed to reduced surface traps on $CuInS_2$ QDs after hybrid passivation, in which iodide ions can remedy the surface defects at the $CuInS_2$ QDs. In contrast, the IPCE values of the solar cells based on ZnS shell coated $CuInS_2$ QDs show a large decrease, and through APCE spectra we found that part of the diminution was induced by the lower loading amount of ZnS shell coated $CuInS_2$ QDs on the TiO_2 film electrodes. However, the ZnS shell coating still cannot improve the APCE values of the

solar cells, and the sample with Zn-10 even exhibited lower APCE than the pristine $CuInS_2$ QDs. To the best of our knowledge, ZnS shell coating has a bifacial effect on $CuInS_2$ QDs. On the one hand, ZnS shell coating can significantly suppress the surface defects on the $CuInS_2$ QDs, and reduce the recombination of the charge carriers in the devices. On the other hand, a ZnS shell will create an electron injection barrier between the $CuInS_2$ QDs and the TiO_2 nanoparticles due to the higher conduction band of ZnS [31]. Some work also indicates that a ZnS shell will decrease the electron transfer (ET) rate, but only slightly reduce the ET efficiency [47].

Current density-voltage (*J-V*) characterization was carried out under the illumination of AM 1.5 G solar simulated light (100 $mW.cm^{-2}$) to evaluate the overall photovoltaic performance of the solar cells based on the different kinds of $CuInS_2$ QDs. Two batches (three parallel cells in each batch) of each kind of $CuInS_2$ QD based QDSCs were fabricated for the measurement. *J-V* curves from the characterization are plotted in Figure 6, and the corresponding PCE, J_{sc}, V_{oc} and FF values are summarized in Figure 7.

Among the four types of $CuInS_2$ QDs, the QDSCs based on hybrid passivated $CuInS_2$ QDs exhibit the highest PCE - a value of 4.7%. Through the comparison we find that the performance improvement of the hybrid passivated $CuInS_2$ QDs based solar cells mainly origins from the enhancement of J_{sc} and V_{oc} of the devices, which amounts to 15.34 mA/cm^2 and 0.560 V, respectively. The increment of J_{sc} can be attributed to two advantages of hybrid passivation of $CuInS_2$ QDs—the improved loading efficiency of the QDs after hybrid passivation, which can increase the light harvesting of the devices; and the promoted quantum efficiency of the QDs, which can enhance the electron injection and collection in the solar cells. The enhancement of V_{oc} should benefit from the suppressed recombination of charge carriers at the interfaces in the devices, which may be referred to reduced surface defects of the hybrid passivated $CuInS_2$ QDs. In contrast, ZnS shell coating makes the PCE of the corresponding solar cells lower than that based on pristine $CuInS_2$ QDs (3.3% and 2.9% for Zn-10 and Zn-20, respectively). The decrease of the performance can mainly be ascribed to the inefficient loading of Zn-10 and Zn-20, leading to a lower photocurrent and a reduced photovoltage. However, the fill factor values of the solar cells based on the coated $CuInS_2$ QDs show improvement over the solar cells based on pristine and hybrid passivated $CuInS_2$ QDs, and a thicker ZnS shell (for Zn-20) has an even higher fill factor value. The fill factor is believed to be influenced by recombination in the devices, and together with the enhanced emission intensity, it demonstrates that ZnS shell coating can indeed eliminate surface traps on the $CuInS_2$ QDs. It follows that a thicker ZnS shell coating has a better effect in this respect. Benefitting from the more suppressed recombination, solar cells based on Zn-20 show higher V_{oc} than that based on Zn-10, though a lower J_{sc} was obtained by the Zn-20 based solar cells.

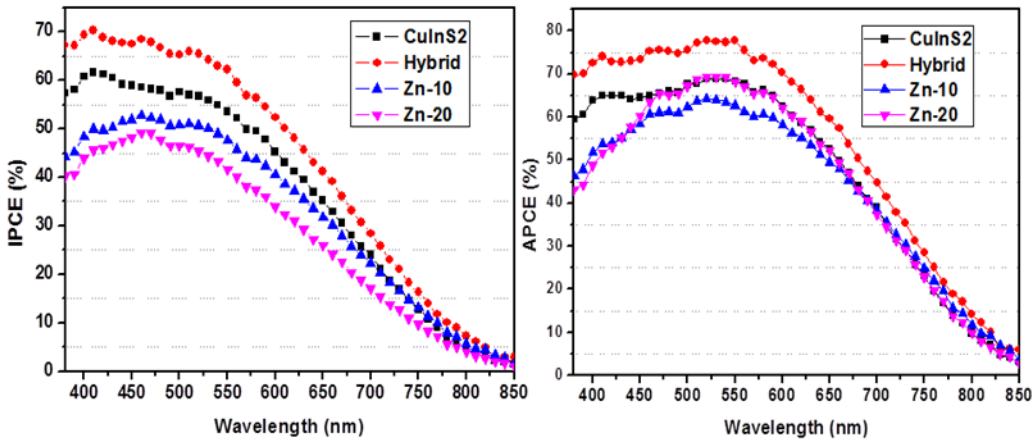

Fig. 5. Incident photon to carrier efficiency (IPCE) and Absorbed photon-to-electron conversion efficiency (APCE) curves of QDSCs based on $CuInS_2$ QDs with different passivation.

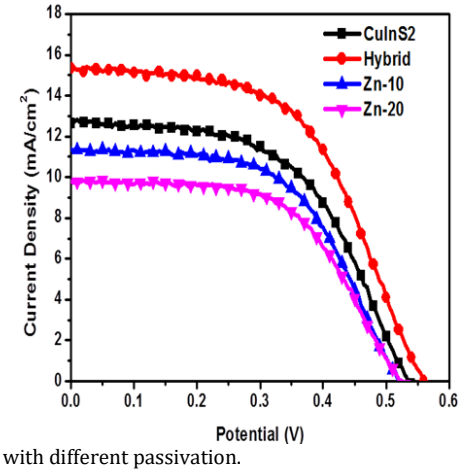

Fig. 6. *J-V* curves of QDSCs based on $CuInS_2$ QDs with different passivation.

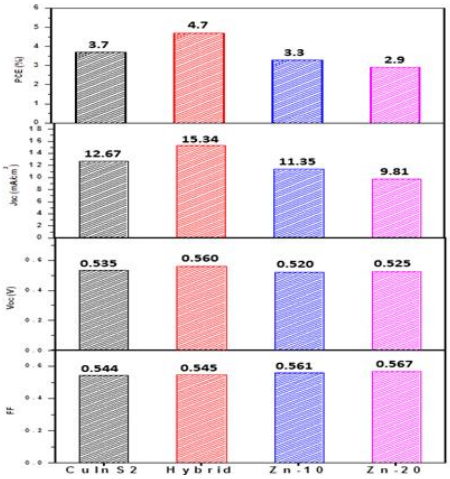

Fig. 7. Photovoltaic parameters (PCE, J_{sc}, V_{oc} and FF) from *J-V* characterization of QDSCs based on $CuInS_2$ QDs with different passivation.

3.5. Impedance spectroscopy

In order to further understand the effects of the passivation strategies on $CuInS_2$ QDs, characterization using impedance spectroscopy (IS) was performed to unveil the recombination resistance in the corresponding solar cells. As illustrated in Figure 8, the solar cells based on the original $CuInS_2$ QDs without any passivation presented the smallest recombination resistance, indicating that charge recombination can easily occur in the devices. Hybrid passivation to the $CuInS_2$ QDs made the recombination resistance in the devices significantly larger, demonstrating that iodide ions in the hybrid passivation treatment can indeed remedy the surface defects on the $CuInS_2$ QDs and suppress the recombination at their surfaces. ZnS shell coating further increased the recombination resistance in the solar cells, and Zn-20 showed a better effect than Zn-10, which indicates that the ZnS shell coating can eliminate the surface defects on $CuInS_2$ QDs to a large extent, and that the recombination in the devices can be better suppressed. We thus find that ZnS shell coating is a more effective surface passivation strategy than hybrid passivation, and that the surface defects on $CuInS_2$ QDs can be better reduced by ZnS shell coating.

Based on our findings in this work, it is worth mentioning that hybrid passivation could increase the solar cell efficiency much better than ZnS shell coating.

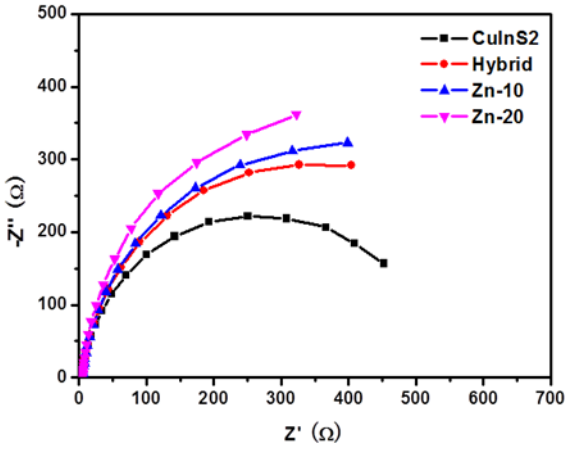

Fig. 8. Nyquist plots from IS measurement of QDSCs based on $CuInS_2$ QDs with different passivation under dark conditions at -0.55 V.

4. Conclusion

Motivated by the need to find "green" alternatives for quantum dot sensitized solar cells (QDSCs), we have in this work employed ZnS shell coating and hybrid passivation to improve the photovoltaic performance of $CuInS_2$ QDs. Hybrid passivation can increase the loading efficiency of QDs on TiO_2 film electrode, promote the electron injection and collection in the devices, and thus improve the photovoltaic performance of $CuInS_2$ QDs in the QDSCs. Though ZnS shell coating of the $CuInS_2$ QDs lower the deposition amount of the QDs and hinders the electron injection from the QDs to the TiO_2 nanoparticles, it can effectively eliminate the surface defects at the $CuInS_2$ QDs. For light emission, our results show that not only ZnS shell coating is a good way to improve the performance for $CuInS_2$ QDs in QDSCs but also that hybrid passivation can be served as a viable way to reach that goal.

Acknowledgements

There is nothing to acknowledgement.

Conflicts of Interest

The author declares that there is no conflict of interest regarding the publication of this article.

References

[1] Minbashi, M. and Yazdani, E., 2022. Effect of Cation and anion migration toward contacts on Perovskite solar cell performance. *Progress in Physics of Applied Materials*, *2*(2), pp.93-102.

[2] Minbashi, M., Ghobadi, A., Ehsani, M.H., Dizaji, H.R. and Memarian, N., 2018. Simulation of high efficiency SnS-based solar cells with SCAPS. *solar energy*, *176*, pp.520-525.

[3] Sahai, S., Jangra, A., Thomas, L.M. and Satsangi, V.R., 2023. Quantum Dots as Efficient Solar Energy Absorber: Review on Photovoltaics and Photoelectrochemical Systems. *Journal of The Institution of Engineers (India): Series D*, pp.1-14.

[4] Ludin, N.A., Mustafa, N.I., Hanafiah, M.M., Ibrahim, M.A., Teridi, M.A.M., Sepeai, S., Zaharim, A. and Sopian, K., 2018. Prospects of life cycle assessment of renewable energy from solar photovoltaic technologies: A review. *Renewable and Sustainable Energy Reviews*, *96*, pp.11-28.

[5] Liu, Z., Lin, C.H., Hyun, B.R., Sher, C.W., Lv, Z., Luo, B., Jiang, F., Wu, T., Ho, C.H., Kuo, H.C. and He, J.H., 2020. Micro-light-emitting diodes with quantum dots in display technology. *Light: Science & Applications*, *9*(1), p.83.

[6] Lohse, S.E. and Murphy, C.J., 2012. Applications of colloidal inorganic nanoparticles: from medicine to energy. *Journal of the American Chemical Society*, *134*(38), pp.15607-15620.

Shen, Y.J. and Lee, Y.L., 2008. Assembly of CdS quantum dots onto mesoscopic TiO_2 films for quantum dot-sensitized solar cell applications. *Nanotechnology*, *19*(4), p.045602.

[8] Jun, H.K., Careem, M.A. and Arof, A.K., 2013. Quantum dot-sensitized solar cells—perspective and recent developments: a review of Cd chalcogenide quantum dots as sensitizers. *Renewable and Sustainable Energy Reviews*, *22*, pp.148-167.

[9] Yang, Z., Chen, C.Y., Roy, P. and Chang, H.T., 2011. Quantum dot-sensitized solar cells incorporating nanomaterials. *Chemical Communications*, *47*(34), pp.9561-9571.

[10] Hanna, M.C. and Nozik, A.J., 2006. Solar conversion efficiency of photovoltaic and photoelectrolysis cells with carrier multiplication absorbers. *Journal of Applied Physics*, *100*(7).

[11] Kamat, P.V., 2013. Quantum dot solar cells. The next big thing in photovoltaics. *The journal of physical chemistry letters*, *4*(6), pp.908-918.

[12] Kwon, Y.T., Choi, Y.M., Kim, K.H., Lee, C.G., Lee, K.J., Kim, B.S. and Choa, Y.H., 2014. Synthesis of CdSe/ZnSe quantum dots passivated with a polymer for oxidation prevention. *Surface and Coatings Technology*, *259*, pp.83-86.

[13] Zhang, J., Li, C., Li, J. and Peng, X., 2023. Synthesis of CdSe/ZnSe Core/Shell and CdSe/ZnSe/ZnS Core/Shell/Shell Nanocrystals: Surface-Ligand Strain and CdSe–ZnSe Lattice Strain. *Chemistry of Materials*, *35*(17), pp.7049-7059.

[14] Jin, N., Sun, Y., Shi, W., Wang, P., Nagaoka, Y., Cai, T., Wu, R., Dube, L., Nyiera, H.N., Liu, Y. and Mani, T., 2023. Type-I CdS/ZnS Core/Shell Quantum Dot-Gold Heterostructural Nanocrystals for Enhanced Photocatalytic Hydrogen Generation. *Journal of the American Chemical Society*, *145*(40), pp.21886-21896.

[15] Zhang, X., Xu, M., YUb, C.H.U.N.M.A.N., LUb, H.A.O., YUb, Y.A.O.T.I.A.N. and XUa, X.I.A.O.N.A.N., 2015. Low temperature aqueous phase synthesis and optical property study of ZnSe/ZnS core/shell quantum dots. *Optoelectronics and Advanced Materials-Rapid Communications*, *9*(July-August 2015), pp.924-929.

[16] Krobkrong, N., Uematsu, T., Torimoto, T. and Kuwabata, S., 2023. Emission tuning of $AgInS_2$-based core/shell semiconductor quantum dots with type-II and quasi-type-II band alignments. *Japanese Journal of Applied Physics*, *62*(6), p.061003.

[17] Liu, J., Yue, S., Zhang, H., Wang, C., Barba, D., Vidal, F., Sun, S., Wang, Z.M., Bao, J., Zhao, H. and Selopal, G.S., 2023. Efficient Photoelectrochemical Hydrogen Generation Using Eco-Friendly "Giant" InP/ZnSe Core/Shell Quantum Dots. *ACS Applied Materials & Interfaces*, *15*(29), pp.34797-34808.

[18] Acharya, K.P., Nguyen, H.M., Paulite, M., Piryatinski, A., Zhang, J., Casson, J.L., Xu, H., Htoon, H. and Hollingsworth, J.A., 2015. Elucidation of two giants: challenges to thick-shell synthesis in CdSe/ZnSe and ZnSe/CdS core/shell quantum dots. *Journal of the American Chemical Society*, *137*(11), pp.3755-3758.

[19] Yahia-Ammar, A., Nonat, A.M., Boos, A., Rehspringer, J.L., Asfari, Z. and Charbonnière, L.J., 2014. Thin-coated water soluble CdTeS alloyed quantum dots as energy

donors for highly efficient FRET. *Dalton Transactions*, *43*(41), pp.15583-15592.

[20] Adegoke, O., Nyokong, T. and Forbes, P.B., 2015. Structural and optical properties of alloyed quaternary CdSeTeS core and CdSeTeS/ZnS core–shell quantum dots. *Journal of Alloys and Compounds*, *645*, pp.443-449.

[21] Sahu, J., Prusty, D., Mansingh, S. and Parida, K., 2023. A review on alloyed quantum dots and their applications as photocatalysts. *International Journal of Hydrogen Energy*.

[22] Siffalovic, P., Badanova, D., Vojtko, A., Jergel, M., Hodas, M., Pelletta, M., Sabol, D., Macha, M. and Majkova, E., 2015. Evaluation of low-cadmium ZnCdSeS alloyed quantum dots for remote phosphor solid-state lighting technology. *Applied Optics*, *54*(23), pp.7094-7098.

[23] Carey, G.H., Levina, L., Comin, R., Voznyy, O. and Sargent, E.H., 2015. Record charge carrier diffusion length in colloidal quantum dot solids via mutual dot-to-dot surface passivation. *Advanced Materials*, *27*(21), pp.3325-3330.

[24] Zhao, K., Pan, Z., Mora-Seró, I., Cánovas, E., Wang, H., Song, Y., Gong, X., Wang, J., Bonn, M., Bisquert, J. and Zhong, X., 2015. Boosting power conversion efficiencies of quantum-dot-sensitized solar cells beyond 8% by recombination control. *Journal of the American Chemical Society*, *137*(16), pp.5602-5609.

[25] Mousavi-Kamazani, M., Salavati-Niasari, M., Hosseinpour-Mashkani, S.M. and Goudarzi, M., 2015. Synthesis and characterization of $CuInS_2$ quantum dot in the presence of novel precursors and its application in dyes solar cells. *Materials Letters*, *145*, pp.99-103.

[26] Guo, F., He, J., Li, J., Wu, W., Hang, Y. and Hua, J., 2013. Photovoltaic performance of bithiazole-bridged dyes-sensitized solar cells employing semiconducting quantum dot $CuInS_2$ as barrier layer material. *Journal of colloid and interface science*, *408*, pp.59-65.

[27] Lv, M., Zhu, J., Huang, Y., Li, Y., Shao, Z., Xu, Y. and Dai, S., 2015. Colloidal $CuInS_2$ quantum dots as inorganic hole-transporting material in perovskite solar cells. *ACS Applied Materials & Interfaces*, *7*(31), pp.17482-17488.

[28] Yue, W., Xie, Z., Pan, Y., Zhang, G., Wang, S., Xu, F., Yao, C., Hu, L., Li, D., Yang, X. and Song, Q., 2015. Improved Device Performance of Polymer-$CuInS_2$/TiO_2 Solar Cells Based on Treated $CuInS_2$ Quantum Dots. *Journal of Electronic Materials*, *44*, pp.3294-3301.

[29] Gardelis, S. and Nassiopoulou, A.G., 2014. Evidence of significant down-conversion in a Si-based solar cell using $CuInS_2$/ZnS core shell quantum dots. *Applied Physics Letters*, *104*(18).

[30] Peng, Z., Liu, Y., Zhao, Y., Chen, K., Cheng, Y., Kovalev, V. and Chen, W., 2014. ZnSe passivation layer for the efficiency enhancement of $CuInS_2$ quantum dots sensitized solar cells. *Journal of alloys and compounds*, *587*, pp.613-617.

[31] Chang, J.Y., Lin, J.M., Su, L.F. and Chang, C.F., 2013. Improved performance of $CuInS_2$ quantum dot-sensitized solar cells based on a multilayered architecture. *ACS applied materials & interfaces*, *5*(17), pp.8740-8752.

[32] Luo, J., Wei, H., Huang, Q., Hu, X., Zhao, H., Yu, R., Li, D., Luo, Y. and Meng, Q., 2013. Highly efficient core–shell $CuInS_2$–Mn doped CdS quantum dot sensitized solar cells. *Chemical Communications*, *49*(37), pp.3881-3883.

[33] Pan, Z., Mora-Seró, I., Shen, Q., Zhang, H., Li, Y., Zhao, K., Wang, J., Zhong, X. and Bisquert, J., 2014. High-efficiency "green" quantum dot solar cells. *Journal of the American Chemical Society*, *136*(25), pp.9203-9210.

[34] Chen, B., Zhong, H., Zhang, W., Tan, Z.A., Li, Y., Yu, C., Zhai, T., Bando, Y., Yang, S. and Zou, B., 2012. Highly emissive and color-tunable $CuInS_2$-based colloidal semiconductor nanocrystals: off-stoichiometry effects and improved electroluminescence performance. *Advanced Functional Materials*, *22*(10), pp.2081-2088.

[35] Uehara, M., Watanabe, K., Tajiri, Y., Nakamura, H. and Maeda, H., 2008. Synthesis of $CuInS_2$ fluorescent nanocrystals and enhancement of fluorescence by controlling crystal defect. *The Journal of chemical physics*, *129*(13).

[36] Kim, Y.K., Ahn, S.H., Chung, K., Cho, Y.S. and Choi, C.J., 2012. The photoluminescence of $CuInS_2$ nanocrystals: effect of non-stoichiometry and surface modification. *Journal of Materials Chemistry*, *22*(4), pp.1516-1520.

[37] Li, L., Pandey, A., Werder, D.J., Khanal, B.P., Pietryga, J.M. and Klimov, V.I., 2011. Efficient synthesis of highly luminescent copper indium sulfide-based core/shell nanocrystals with surprisingly long-lived emission. *Journal of the American Chemical Society*, *133*(5), pp.1176-1179.

[38] Zhang, W. and Zhong, X., 2011. Facile synthesis of ZnS– $CuInS_2$-alloyed nanocrystals for a color-tunable fluorchrome and photocatalyst. *Inorganic chemistry*, *50*(9), pp.4065-4072.

[39] Park, J. and Kim, S.W., 2011. $CuInS_2$/ZnS core/shell quantum dots by cation exchange and their blue-shifted photoluminescence. *Journal of Materials Chemistry*, *21*(11), pp.3745-3750.

[40] Li, T.L., Lee, Y.L. and Teng, H., 2011. $CuInS_2$ quantum dots coated with CdS as high-performance sensitizers for TiO_2 electrodes in photoelectrochemical cells. *Journal of Materials Chemistry*, *21*(13), pp.5089-5098.

[41] Hu, X., Zhang, Q., Huang, X., Li, D., Luo, Y. and Meng, Q., 2011. Aqueous colloidal $CuInS_2$ for quantum dot sensitized solar cells. *Journal of Materials Chemistry*, *21*(40), pp.15903-15905.

[42] McDaniel, H., Fuke, N., Makarov, N.S., Pietryga, J.M. and Klimov, V.I., 2013. An integrated approach to realizing high-performance liquid-junction quantum dot sensitized solar cells. *Nature communications*, *4*(1), p.2887.

[43] Tang, J., Kemp, K.W., Hoogland, S., Jeong, K.S., Liu, H., Levina, L., Furukawa, M., Wang, X., Debnath, R., Cha, D. and Chou, K.W., 2011. Colloidal-quantum-dot photovoltaics using atomic-ligand passivation. *Nature materials*, *10*(10), pp.765-771.

[44] Ip, A.H., Thon, S.M., Hoogland, S., Voznyy, O., Zhitomirsky, D., Debnath, R., Levina, L., Rollny, L.R., Carey, G.H., Fischer, A. and Kemp, K.W., 2012. Hybrid passivated colloidal quantum dot solids. *Nature nanotechnology*, *7*(9), pp.577-582.

[45] Huang, J., Xu, B., Yuan, C., Chen, H., Sun, J., Sun, L. and Ågren, H., 2014. Improved performance of colloidal CdSe quantum dot-sensitized solar cells by hybrid passivation. *ACS applied materials & interfaces*, *6*(21), pp.18808-18815.

[46] Li, W. and Zhong, X., 2015. Capping ligand-induced self-assembly for quantum dot sensitized solar cells. *The journal of physical chemistry letters*, *6*(5), pp.796-806.

[47] Sun, J. Zhao, J. and Masumoto, Y., 2013. Shell-thickness-dependent photoinduced electron transfer from $CuInS_2$/ZnS quantum dots to TiO_2 films. *Applied physics letters*, *102*(5).